Infrared Physics & Technology 76 (2016) 315–327

Contents lists available at ScienceDirect

Infrared Physics & Technology

journal homepage: www.elsevier.com/locate/infrared

Structural and spectroscopic study of a pectin isolated from citrus peel by using FTIR and FT-Raman spectra and DFT calculations

Laura C. Bichara [a], Patricia E. Alvarez [b,c], María V. Fiori Bimbi [b], Hugo Vaca [b], Claudio Gervasi [c], Silvia Antonia Brandán [a,*]

[a] Cátedra de Química General, Instituto de Química Inorgánica, Facultad de Bioquímica, Química y Farmacia, Universidad Nacional de Tucumán, Ayacucho 471, 4000 San Miguel de Tucumán, Tucumán, Argentina
[b] Cátedra de Física I, Instituto de Física, Facultad de Bioquímica, Química y Farmacia, Universidad Nacional de Tucumán, Ayacucho 471, 4000 S.M. de Tucumán, Argentina
[c] Instituto de Investigaciones Fisicoquímicas Teóricas y Aplicadas (INIFTA), Facultad de Ciencias Exactas., Suc. 4, C.C. 16, LIMF, Facultad de Ingeniería, UNLP, Calle 48 y 116, 1900 La Plata, Argentina

HIGHLIGHTS

- Pectin isolated from citrus peel was characterized by IR and Raman spectra.
- The polygalacturonic acid chain was characterized by using two proposed structures.
- The complete assignments of the two structures proposed were performed.
- Both structures were studied by using NBO, AIM and frontier orbitals calculations.
- This study provides new insight to study the interactions of a pectin chain.

GRAPHICAL ABSTRACT

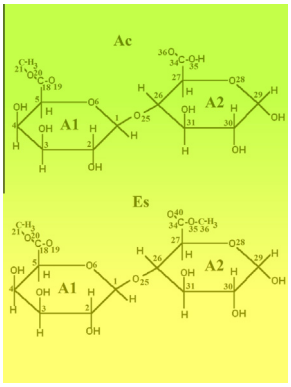

ARTICLE INFO

Article history:
Received 13 February 2016
Revised 13 March 2016
Accepted 14 March 2016
Available online 15 March 2016

Keywords:
Pectin
Vibrational spectra
Molecular structure
Force field
DFT calculations

ABSTRACT

In this work, pectin isolated from citrus peel with a degree of esterification of 76% was characterized by Fourier Transform Infrared (FTIR) and Fourier Transform Raman (FT-Raman) spectroscopies. Structural studies were carried out taking into account their partial degree of esterification and considering the polygalacturonic acid chain as formed by two different subunits, one with both COOH and COO—CH_3 groups (Ac) and the other one as constituted by two subunits with two COO—CH_3 groups (Es). Their structural properties, harmonic frequencies, force fields and force constants in gas and aqueous solution phases were calculated by using the hybrid B3LYP/6-31G* method. Then, their complete vibrational analyses were performed by using the IR and Raman spectra accomplished with the scaled quantum mechanical (SQM) methodology. Reactivities and behaviors in both media were predicted for Ac and Es by using natural bond orbital (NBO), atoms in molecules (AIM), and frontier orbitals calculations. We report for first time the complete assignments of those two different units of polygalacturonic acid chain which are the 132 normal vibration modes of Ac and the 141 normal vibration modes of Es, combining the normal internal coordinates with the SQM methodology. In addition, three subunits were also studied. Reasonable correlations between the experimental and theoretical spectra were obtained. Thus, this work

* Corresponding author.
E-mail address: sbrandan@fbqf.unt.edu.ar (S.A. Brandán).

http://dx.doi.org/10.1016/j.infrared.2016.03.009

would allow the quick identification of pectin by using infrared and Raman spectroscopies and also provides new insight into the interactions that exist between subunits of a large pectin chain.

1. Introduction

Pectin substances are of great interest in the chemical, nutrition and pharmaceutical industries because due to their gelling properties they are employed in multiple applications in such as in production of citrus juices, jams and jellies, as a carrier for drug delivery to the gastrointestinal tract, as matrix tablets, gel beads and film-coated dosage forms [1–5]. From a chemical point of view, pectin can be described as a linear polysaccharide where the subunits of a molecule are different from those other molecule because their structures depend on the esterification degree during extraction from citrus peels [1,5]. Although pectin was discovered long time ago even their composition and structure remain unresolved [1]. In three different preparations of pectins Kravtchenko et al. [4] have found that all the structures are slightly acetylated while Synytsya et al. [6] have reported a vibrational study on the polygalacturonic (pectic) acid, potassium pectate and its derivatives, as well as on commercial citrus and sugar beet pectins. These authors have recorded and interpreted only some bands observed in the corresponding infrared and Raman spectra of those samples but, they have not performed the vibrational assignments taking into account the corresponding structures [6]. In this context and, knowing that galacturonic acid units constitute the chain of this carbohydrate polymer, and, that the units are linked among them by α-1,4-D-glycosidic bonds, as reported for disaccharides like sucrose and lactose and for a sweetener like sucralose [7–9], we have performed this work to investigate the structures of two different units of galacturonic acid based on the complete vibrational assignment of the infrared and Raman spectra of a pectin isolated from citrus peel with a degree of esterification of 76% [10]. Therefore, the goal of this paper is to perform a structural and vibrational study of this pectin considering the structure of the polygalacturonic acid chain as formed, first by two different subunits with both COOH and COO—CH_3 groups and, then, as constituted by two subunits with two COO—CH_3 groups. Thus, for these two cases we took into account esterification degrees of approximately 50% and 100%, respectively. Hence, the initial structures of those forms were optimized by using the hybrid B3LYP/6-31G* method [11,12] in gas phase and in aqueous solution [13,14] and, afterward their harmonic frequencies and force fields were calculated by using the normal internal coordinates and the SQM procedure in order to perform the complete assignments of all the normal vibration modes of both forms considered [15]. Additionally, three subunits formed by two COO—CH_3 groups and one COO group were theoretically simulated in order to compare their corresponding infrared and Raman spectra with those obtained for the two different proposed structures with two subunits described above. In the case of three subunits the system represents pectin esterified to a degree of approximately 70%. Here, our results were compared with those reported for the group of pectins studied by Synytsya et al. [6]. Later, the structural and vibrational properties were compared and discussed in relation to those obtained in aqueous medium. In addition, the force constants were also reported for the main groups and compared with similar data reported in the literature [7–9]. The simulated vibrational spectra for the structures here proposed show a reasonable correlation with the corresponding experimental data for which these structures are useful to study the polygalacturonic acid chain that forms the pectin molecule. Hence, this work provides new insight into the interactions that exist between subunits of a large pectin chain and, in addition, this work would allow a quick identification of pectin by using the vibrational spectroscopy.

2. Experimental methods

The pectin was isolated from citrus peel with a degree of esterification of 76% according to procedure explained in the previous studies [10]. The FTIR spectrum of the compound in solid phase was recorded with the KBr pellet technique in the region 4000–400 cm^{-1} with an FT-IR Perkin Elmer spectrophotometer, equipped with a Globar source and a DGTS detector. The FT-Raman spectrum of the sample was obtained in the range 4000–50 cm^{-1} using Bruker RFS 100/s FT-Raman spectrophotometer with a 1064 nm Nd: Yag laser source of 150 mW power. Spectra were recorded with a resolution of 1 cm^{-1} and 200 scans.

3. Computational details

Two different subunits of the polygalacturonic acid, one with COOH and COO—CH_3 groups (**Ac**) and the other one constituted by two subunits with two COO—CH_3 groups (**Es**) were initially modeled by the *GaussView* program [16]. Then, these structures were optimized in gas and aqueous solution phases by using the hybrid B3LYP/6-31G* method [11,12]. In solution, the solvent effects were considered by using the PCM model [13,14] while the SM model [17] was employed to obtain the corresponding solvation energies for the two structures, as in similar systems studied in solution [9,18,19]. Here, all the calculations in gas and in solution were performed by using the Gaussian program [20]. Besides, three subunits formed by two COO—CH_3 and one COOH groups were also simulated and optimized in both media. The structures for the two first **Ac** and **Es** systems can be seen in Fig. 1 while Fig. 2 shows the optimized structure for three subunits of pectin. Here, the molecular electrostatic potential, atomic charges, stabilization energy values, topological properties and gap energies for **Ac** and **Ec** were studied by using NBO [21,22], AIM [23,24] and HOMO–LUMO [25] calculations in order to predict their reactivities and behaviors in both media. The Merz–Kollman (MK) charges were also calculated from the molecular electrostatic potential, according to the Merz–Kollman scheme [26]. The force fields for **Ac** and **Ec** in both media were computed at the theory level using the Cartesian coordinates by using the SQM procedure and the Molvib program [27]. Then, this latter program was also used to transform the resulting force fields in Cartesian coordinates to normal internal coordinates. The definition of these coordinates for **Ac** and **Ec** are summarized in Tables S1 and S2 (Supporting material) and they were constructed according to similar systems [8,9]. To perform the complete vibrational assignments of **Ac** and **Ec** were considered contributions with the potential energy distribution (PED) $\geqslant$ 10% but, only for some modes a 7% contribution were considered. For the system of three units the assignment was performed with the aid of the *GaussView* program [16].

4. Results and discussion

4.1. Geometry optimization

Table S3 shows the calculated total energy, dipolar moments, molecular volume and solvation energies for the two **Ac** and **Ec**

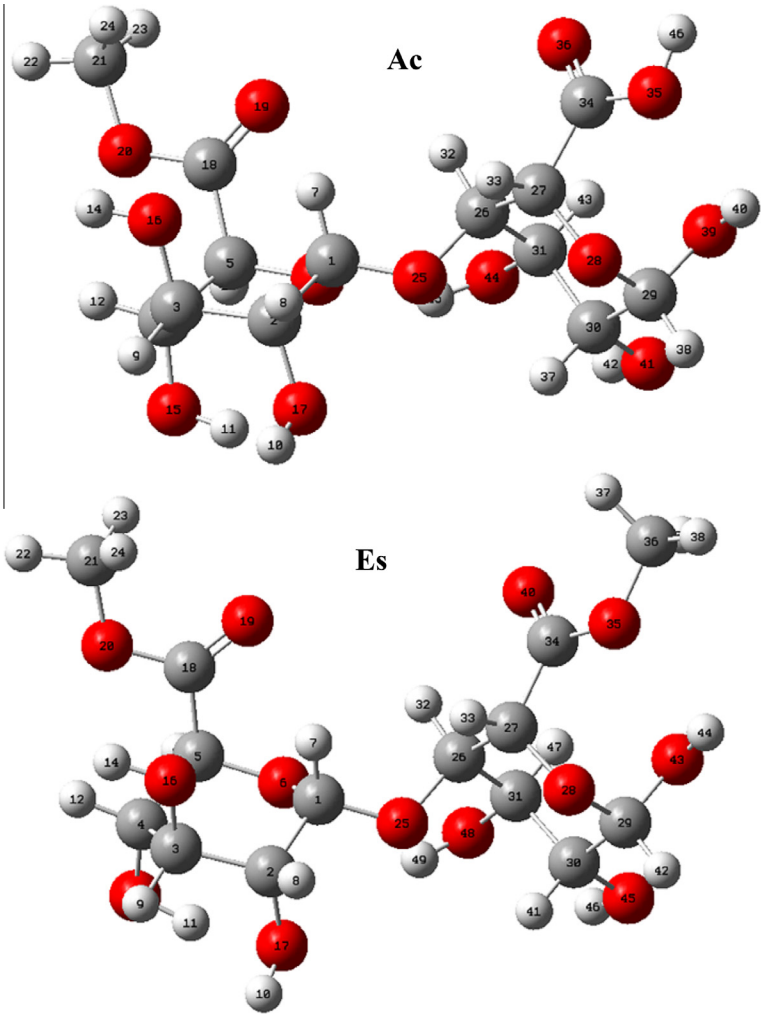

Fig. 1. Theoretical molecular structures of two units of the galacturonic acid for a: (a) pectin acid, Ac (upper) and (b) pectin esterified, Es, (bottom) together with the atoms numbering.

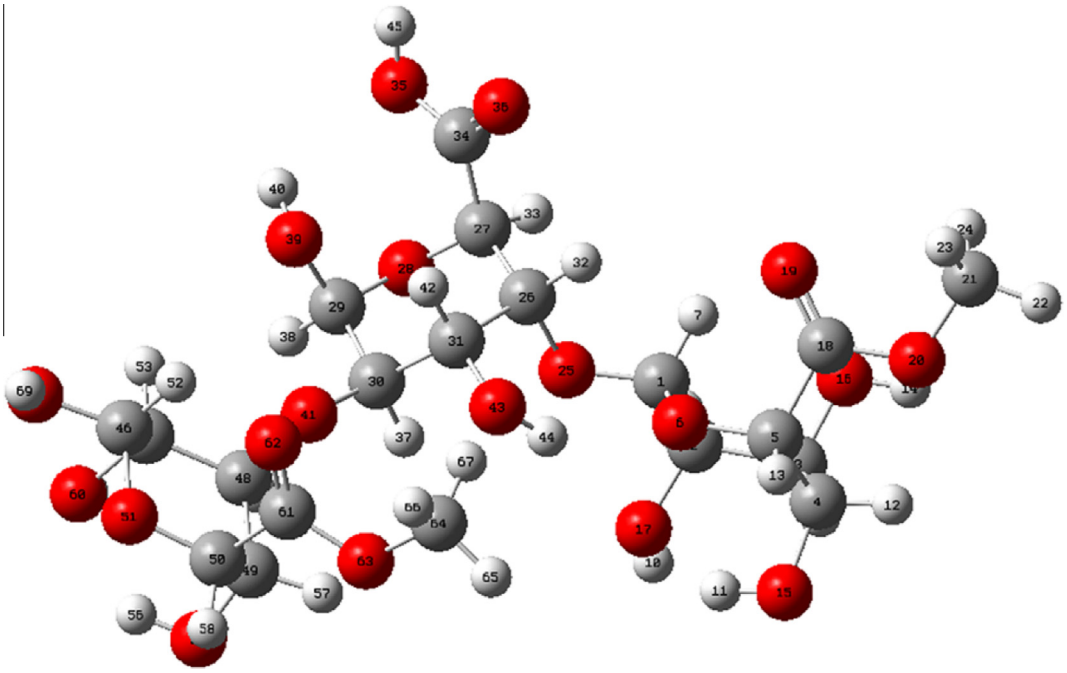

Fig. 2. Theoretical molecular structure of three units of the galacturonic acid of acid and esterified pectin together with the atoms numbering.

forms of pectin studied. Note that the dipole moment value for **Ac** in gas phase is greater than the value corresponding to **Es** in the same medium but, in solution a contrary result is obtained as a consequence of the hydration of the OH and COO groups. Thus, the orientation and magnitude of the dipole moments for both forms change notably in solution due to the hydration of the OH and COO groups of both forms by hydrogen bonding (H bonds) formation. Probably, the higher value in solution for **Es** is related to the presence of a CH_3 group linked to a COO group that decreases the solvation, in relation to **Ac**, as suggested by the volume and solvation energy values. The volume variations, calculated by the Moldraw program [28] reveal a higher hydration for **Ac**, as supported by the high solvation energy value. Here, the solvation energy values uncorrected (ΔG_{un}) are the energy variations between the values in solution and in gas phase while the corrected values (ΔG_C) are those calculated taking into account the non-electrostatic terms by using the universal solvation model [17–19]. Fig. S2 shows the disposition of all the atoms in the two proposed structures and the names of both rings together with the corresponding α-1,4-D-glycosidic bonds. On the other hand, the comparisons of the theoretical geometrical parameters of **Ac** and **Ec** with those experimental ones determinate for methyl-α-D-galacturonic acid methyl ester by Lamba et al. [29] and with some values calculated for sucrose [9] by means of the root-mean-square deviation (RMSD) are given in Table 1. The results show a better correlation for bond length (0.027–0.021 Å) and angles (1.8–1.6°) than for the dihedral angles (18.4–14.6°). Note that in solution the bond angles for **Ac** are slightly higher than **Es**, as expected due to their higher solvation. Clearly, the differences observed between the calculated and experimental values can be in part attributed to the calculations because they were computed in gas phase for the isolated molecules without regard to the crystal packing chain. In the two structures, the glycosidic C1—O25 bond is calculated with lower values in both media than the other ones while a contrary result is observed for the C1—O26 bonds. On the other hand, the glycosidic C1—O25—O26 angle in both structures is predicted with low values in relation to the experimental ones. Moreover, in solution the dihedral angles for **Es** decrease while for **Ac** slightly increases in this medium show that the presence of two CH_3 groups justify the low hydration of that structure in aqueous solution, as supported by the volume variation and solvation energies.

4.2. Electrostatic potential, charges types and bond orders

For the two **Ac** and **Ec** structures proposed both the charges and the molecular electrostatic potential (MEP) were calculated because these properties are of importance to localize the electrophilic and nucleophilic regions taking into account that in these sites occur the H bonds formation in solution. Thus, in Table S4 are presented the calculated molecular electrostatic potential of **Ac** and **Ec** by using the B3LYP/6-31G* method in both media. Obviously, the highest values are observed on the O41 and O44 atoms of **Ac** and on the O45 and O48 atoms of **Ec** in both media probably

Table 1
Comparison of calculated geometrical parameters for the two proposed pectins with the corresponding experimental ones for methyl-α-D-galacturonic acid methyl.

B3LYP/6-31G*[a]					Exp.[b]
Parameters	Ac		Es		
	Gas	Solution	Gas	Solution	
Bond lengths (Å)					
C1—O6	1.441	1.437	1.432	1.437	1.423
C5—O6	1.420	1.425	1.418	1.422	1.423
C1—O25	1.382	1.398	1.388	1.398	1.438[c]
C26—O25	1.445	1.443	1.445	1.444	1.417[c]
C27—O28	1.421	1.430	1.423	1.428	1.423
C29—O28	1.430	1.430	1.428	1.429	1.423
C18—O19	1.208	1.218	1.208	1.218	1.191
C18—O20	1.352	1.339	1.353	1.337	1.320
C34—O36	1.210	1.218	1.210	1.219	1.191
C34—O35	1.356	1.344	1.350	1.338	1.320
RMSD	0.027	0.021	0.024	0.021	
Bond angles (°)					
C1—O25—C26	116.6	114.9	115.5	115.1	118.9[c]
C1—O6—C5	114.7	114.7	114.1	114.4	112.4
C27—O28—C29	115.0	114.9	114.9	114.3	112.4
O20—C18—O19	123.9	124.0	123.8	124.0	124.7
O36—C34—O35	122.5	123.3	123.6	124.0	124.7
C18—O20—C21	115.1	116.2	115.1	116.2	116.8
C5—C18—O20	110.4	111.2	110.7	111.7	110.4
C5—C18—O19	125.4	124.6	125.3	124.1	124.8
C27—C34—O35	112.7	111.8	111.9	111.4	110.4
C27—C34—O36	124.4	124.5	124.1	124.2	124.8
RMSD	1.8	1.8	1.7	1.6	
Dihedral angle (°)					
C5—C18—O20—C21	−175.7	−177.5	−175.7	−177.6	−178.8
O6—C1—O25—C26	77.2	76.1	70.6	74.4	107.8[c]
O25—C26—C27—O28	68.4	68.0	67.6	67.5	
C2—C1—O25—C26	−163.4	−163.5	−169.7	−164.9	−152.4[c]
RMSD	14.6	15.0	18.4	16.0	

[a] This work.
[b] From Ref. [28].
[c] From Ref. [9].

because these atoms are linked to H atoms that are involved in intramolecular H bonds while these values decrease in solution, with exception of the O48 atom, as a consequence of the hydration. On the contrary, the MEP values on the O atoms belonging to the COO groups of both structures for the same reason increase slightly their values in solution. The less negative MEP values are observed on the H10, H11, H14 and H46 atoms of **Ac** and on the H10, H11, H14 and H44 atoms of **Ec** in both media possibly because these two latter atoms are forming intramolecular H bonds with the O35 and O25 atoms, respectively. The mapped electrostatic surfaces for both structures in gas phase can be seen in Fig. S3 and they show that the nucleophilic regions, identified by the red colours, are localized on the O atoms belonging to the C=O bonds and to the OH groups while the electrophilic regions identified by the blue colours are clearly localized on the H atoms with low MEP values in both structures. Thus, the different colorations reveal clearly the diverse regions.

Two charges types were studied for **Ac** and **Es** in both media which are the MK and natural population atomic (NPA) charges whose calculated values can be seen in Table S5. The analyses of the same show that: (i) the NPA charges have in general higher values than the other ones, (ii) both charges have different behaviors in solution, it is, in some cases increase the values while in other decrease, (iii) the NPA charges on the O19 and O36 atoms of **Ac** and on the O19 and O40 atoms of **Es** belonging to the C=O bonds increase their values in solution due to the hydration but, the MK charge values on the H19 atoms for both forms decrease in solution, (iv) the NPA charges on the O atoms linked to the CH_3 groups decrease in solution while the MK charges do not show a defined tendency, (v) the MK charges on the C18 and C34 atoms belonging to the COO groups of both structures exhibit different values, as expected because in Ac those groups are linked to OH and CH_3 groups but in **Es** both C atoms are linked to CH_3 groups, (vi) the MK charges on the C atoms of the COO groups show low values when these groups are not esterified, as in Ac while have similar values when are esterified, as in Es and, finally, (vii) the MK charges on the COO groups show clear differences between the two structures in solution.

To understand the behaviors of both proposed species in solution it is necessary to study the bond orders because in solution these values decrease due to the H bonds formation, as compared with the corresponding values in gas phase, thus, the H bonds formation clearly take places. For this reason, for both structures the bond order values in the two media are presented in Table S6. Effectively, the exhaustive analysis show that the higher values are observed for the O atoms corresponding to the COO groups of both forms, thus, the decreasing the these values in solution suggest the H bonds formation in solution in both structures. On the other hand, the increasing in the bond orders values of the O atoms of OH groups in both forms also suggest the clear hydration of these groups in solution.

4.3. NBO study

The main delocalization energy for the two proposed structures of pectin were calculated in order to study the stabilities of both forms in gas phase and in aqueous solution by using the NBO calculations [21,22] and the B3LYP/6-31G* method. The results in both media are presented in Table S7. Thus, the Ac structure show a high stability due to the presence of three $\Delta E_{n\rightarrow\sigma*}$, $\Delta E_{n\rightarrow\Pi*}$ and $\Delta E_{\sigma*\rightarrow\sigma*}$ charge transfers that generate an ΔE_{Total} higher in gas phase than in solution. These delocalization energies are related to the lone pairs of the O atoms belonging to the C=O and OH bonds of the COOH groups and to the lone pairs of the O atoms belonging to the OH groups of both rings. These stabilization energies in both media are higher in **Ac** than **Es**, being higher in aqueous solution. Note that for both forms the $\Delta E_{n\rightarrow\Pi*}$ charge transfers in both media are associated with the lone pairs of the O20 and O35 atoms of the C34—O35—H46 and C18—O20—C21 groups in **Ac** and with the lone pairs of the O atoms of the two C—O—C esterified groups in **Es**. Hence, these stabilization energies in both media are higher in **Es** than **Ac**, being higher in solution. This study evidences clearly the higher stabilities of **Ac** in both media than **Es**, suggesting this way, that a structure with both COOH and COO—CH_3 groups is most stable than that with two COO—CH_3 groups, as supported maybe by the higher dipole moment value in gas phase and a higher solvation energy in solution.

4.4. AIM analysis

The Bader's atoms in molecules (AIM) theory [23] is useful to study the inter and intra-molecular interactions or the H bond interactions of different systems especially when in the structures there are atoms that can act as donor o acceptor of H bonds, as in the two proposed **Ac** and **Es** structures which have OH, COOH and COO—CH_3 groups. In this study, the AIM2000 program was used to calculate the topological properties for both species in gas phase and in solution [24]. Table S8 shows the results for both species in the bond critical points (BCPs) at B3LYP/6-31G* levels of theory in gas and aqueous solution phases. Thus, the parameters more important in this study are, the electron density distribution, $\rho(r)$ in the BCPs, the values of the Laplacian, $\nabla^2\rho(r)$, the eigenvalues ($\lambda1$, $\lambda2$, $\lambda3$) of the Hessian matrix at these points and, the $\lambda1/\lambda3$ ratio. This latter ratio allows the description of the character of interaction between atoms. Thus, when $\lambda1/\lambda3 > 1$ and $\nabla^2\rho(r) < 0$ the interaction is typical of covalent bonds (called shared interaction) with high values of $\rho(r)$ and $\nabla^2\rho(r)$ while when $\lambda1/\lambda3 < 1$ and $\nabla^2\rho(r) > 0$ the interaction is called closed-shell interaction and is typical of ionic, highly polar covalent and hydrogen bonds as well as of the van-der-Waals and specific intermolecular interactions, as explained by Bushmarinov et al. [30]. For **Ac** in gas phase we observed four different interactions, three H bonds typical and a C···O interaction while for **Es** are observed five interactions, three of which are H bonds and the remains are O···O and C···O interactions. Figs. S4 and S5 show the BCP and ring critical points (RCPs) for **Ac** and **Es**, respectively in gas phase at the B3LYP/6-31G* level of theory. All these interactions have different properties, as observed in Table S8, having the O17···H11 interactions in **Ac** and **Es** the higher values. Note that in solution the number of H bonds is reduced up to 3 in **Ac** and up to 4 in **Es**. Thus, this study show clearly that some intramolecular interactions disappear in both structures in solution while probably new H bonds can be formed as consequence of the hydration of the **Ac** and **Es** with molecules of the solvent.

4.5. Frontier HOMO–LUMO orbitals

The NBO and AIM calculations have showed that there are differences significant between both structures in the two media studied. Thus, the charges transfers in **Ac** confer to it an energetically high stability than **Es** while, the AIM studies show a higher number of interactions in **Es** in both media than **Ac**. In this sense, it is necessary predict the reactivities and behaviors of both species in the two media. For this reason, the frontier orbitals were calculated taking into account the definition reported by Parr and Person [25]. The calculated values for both forms in the two media can be seen in Table S9. The values show newly clear differences between Ac and Es, thus **Ac** in most reactive in gas phase than **Es** while a contrary result is observed in solution because the reactivity of **Ec** increase in solution. This result support the high stability of Ac by NBO analysis but is not in agree with the higher solvation

energy value of **Ac**. Probably the higher value of the dipole moment value of **Es** in solution is justified by the higher H bonds formation.

4.6. Vibrational analysis

The optimized **Ac** and **Es** structures have C_1 symmetries and 132 and 141 vibration normal modes, respectively and where all vibrations are IR and Raman active. Fig. 3 shows a comparison between the experimental infrared and Raman spectra of the used pectin in solid phase in the 4000–400 and 4000–10 cm^{-1} regions while Figs. 4–6 show the comparisons of these spectra with the corresponding predicted for **Ac** and **Es** in both media at B3LYP/6-31G* level in three different regions. The comparisons among the experimental and theoretical spectra were performed taking into account the 4000–2500, 2000–1000 and 1000–0 cm^{-1} regions. The observed and calculated wavenumbers are summarized in Table 2 together with the proposed assignments for the two structures studied and a comparison with the reported for other pectins [6]. The assignments were performed at the B3LYP/6-31G* level of theory using the SQMFF procedure and the scale factors taken from Ref. [15] and taking into account the PED contribution calculated $\geqslant$10%. The force fields for both structures were calculated at the same level of theory with the Molvib program [27]. On the other hand, the observed and calculated wavenumbers, potential energy distribution and assignments for Ac and Es in gas phase are presented in Tables S10 and S11. Fig. S6 shows a comparison between the experimental IR spectrum of pectin in solid state with those corresponding to the two proposed units, **Ac** and **Es**, in gas phase and in aqueous solution at B3LYP/6-31G* level while Fig. S7 shows a comparison between the experimental IR spectrum of pectin in solid state with that corresponding to three proposed units of the galacturonic acid in gas phase and in aqueous solution at B3LYP/6-31G* level. It is important to observe that the IR spectra predicted for the structure with three units of the galacturonic acid has the same form than those proposed for two units of the acid.

4.6.1. 4000–2500 cm^{-1} region

In this region for **Ac** and **Es** are expected the CH_3 antisymmetric and symmetric, CH and OH stretching modes, as seen in Table 2. From Fig. 4 it is observed that both experimental and theoretical IR and Raman spectra show some bands in two zones. There are one region between 4000 and 3000 cm^{-1} and the other one between 3000 and 2500 cm^{-1}. Also, Tables S10 and S11 show

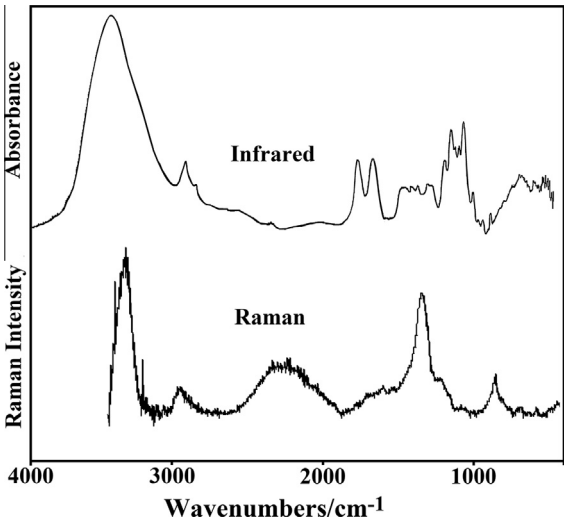

Fig. 3. Comparison between the experimental infrared and Raman spectra of pectin in solid phase in KBr pellet.

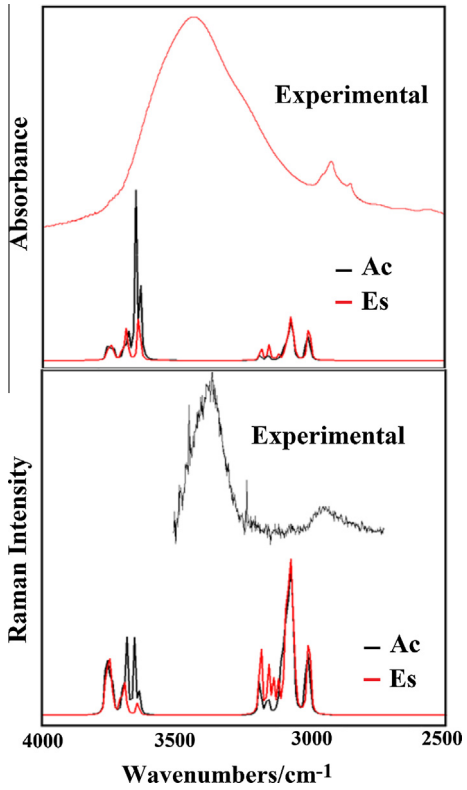

Fig. 4. Comparison between the experimental IR and Raman spectra of pectin in solid state in the 4000–2500 cm^{-1} region with that corresponding to the two proposed units of the galacturonic acid for a pectin acid, Ac and pectin esterified, Es, in gas phase at B3LYP/6-31G* level.

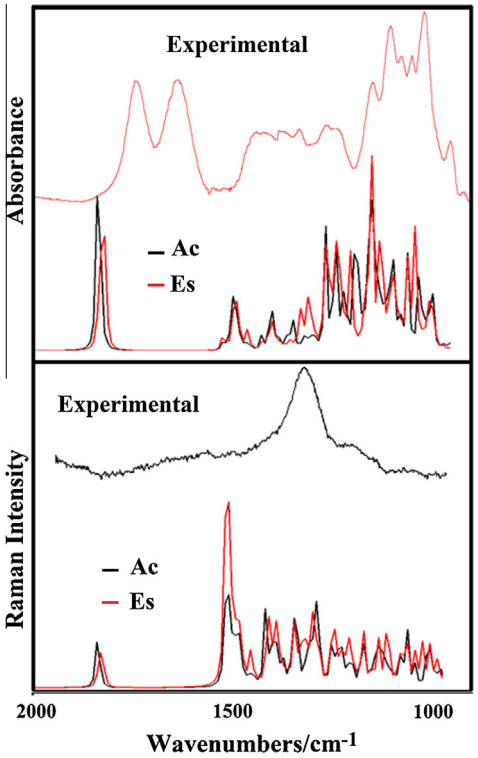

Fig. 5. Comparison between the experimental IR and Raman spectra of pectin in solid state in the 2000–1000 cm^{-1} region with that corresponding to the two proposed units of the galacturonic acid for a pectin acid, Ac and pectin esterified, Es, in gas phase at B3LYP/6-31G* level.

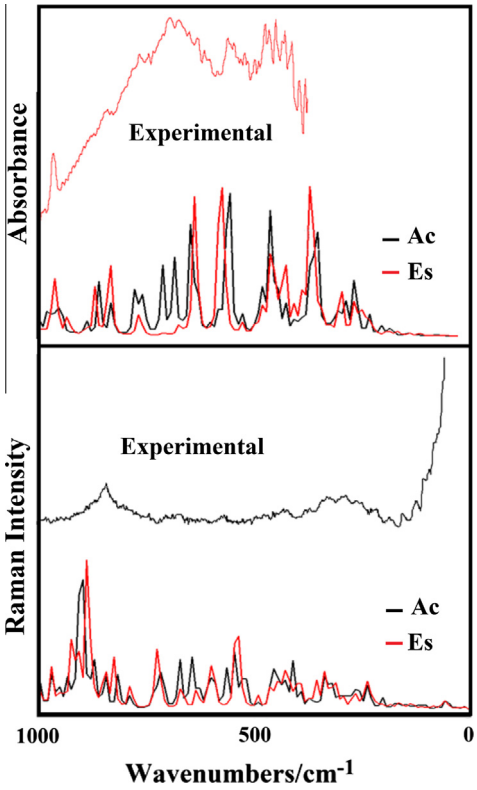

Fig. 6. Comparison between the experimental infrared spectra of pectin in solid state in the 1000–10 cm^{-1} region with that corresponding to the two proposed units of the galacturonic acid for a pectin acid, Ac and pectin esterified, Es, in gas phase at B3LYP/6-31G* level.

approximately that all the modes are predicted by SQM calculations in this region with PED 100% contributions. Then, the intense IR band at 3436 cm^{-1} is easily assigned to OH stretching modes of both **Ac** and **Es** structures and due to the intensity of this band can be clearly associated to the vibration modes of **Ac**, as shown in Figs. 3 and 4. On the contrary, the broad band in the Raman spectrum at 2947 cm^{-1}, of lower intensity than the above band, can be assigned to the symmetric CH_3 stretching modes of both forms but, due to their intensity is principally related to **Es** because this form has two CH_3 groups. Obviously, the remained bands observed in this region are assigned to the antisymmetric CH_3 and C—H stretching modes of **Ac** and **Es**, as indicated in Table 2. In different pectins only two bands were previously reported in this region [6], as can be seen in Table 2. Here, the predicted bands for the proposed structure with three units of the galacturonic acid are presented in Table 2 and, they appear at higher wavenumbers than the other ones because they were not scaled. Notice that for this form of pectin the assignments of the bands to the vibration modes are in accordance with those performed for the two units proposed.

4.6.2. 2000–1000 cm^{-1} region

This region is very difficult to assign because in both species are expected the C=O, C—O and C—C stretching modes, the OH deformation and antisymmetric and symmetric CH_3 deformation modes and the CH_3 and C—H rocking modes. Experimentally, two intense bands between 1800 and 1500 cm^{-1} are observed in the IR spectrum of pectin while in the corresponding Raman spectrum only very weak bands can be observed Clearly, these two bands should be attributed to COO groups with different moieties linked to these which are —OH and —O—CH_3. Therefore, analyzing first the COO groups, we know that when the COO group is anionic, it forms a salt, as in the chromyl acetate [31,32]. The antisymmetric and symmetric C=O stretching modes are observed as two intense bands with a separation between them of about 200 cm^{-1} while the separation between these modes increase notably in amino acids such as, tyrosine, tryptophan, threonine up to 470 cm^{-1} [33–35] and, in acetic acid derivatives compounds the separations are from 400 to 600 cm^{-1}.[36–39]. In this case, the two **Ac** and **Es** structures proposed have each two acetate neutral groups, as in the acetic acid derivatives. Hence, taking into account the corresponding PED contributions those COO—H modes in **Ac** are associated with the strong IR bands at 1743 and 1146 cm^{-1} while those modes related to COO—CH_3 are attributed to the IR bands at 1640 and 1235 cm^{-1}, as indicated in Table 2. In **Es**, according to SQM calculations, the IR bands at 1743/1640 and 1235/1211 cm^{-1} are assigned to the C=O stretching modes of both COO—CH_3 groups. On the other hand, the very weak IR band at 1588 cm^{-1} only can be associated to a C=O stretching mode of a pectin chain, as predicted the calculations for the proposed structure with three units of the galacturonic acid. According to SQM calculation (Tables S10 and S11), the antisymmetric and symmetric CH_3 deformation modes in this region [39–42] are calculated as pure modes while the CH rocking modes are calculated coupled with other similar modes, thus, the former modes can be assigned to the IR and Raman bands between 1460 and 1420 cm^{-1} while the second ones can be attributed to the bands between 1452 and 1191 cm^{-1}. The SQM calculations for **Ac** and **Es** predicted the CH_3 rocking modes between 1192 and 1146 cm^{-1} and, for this reason, these modes were assigned in that region. In **Ac** and **Es**, the OH deformation modes are predicted by SQM calculations with low intensities and PED contribution (34–16%) in the 1440 and 1040 cm^{-1} region, hence, these modes are assigned as indicated in Table 2. Note that in aqueous solution these modes appear at lower wavenumbers due to the hydration by H bonds formation, such as the δO5—H11 mode in **Ac** that in gas phase is assigned at 1440 cm^{-1} while in solution it is predicted at 1280 cm^{-1}. On the other hand, the C—O stretching for **Ac** and **Es** are predicted by calculations with high intensities and, for this reason, the bands at 1235, 1146, 1103, 1076, 1047 and 1017 cm^{-1} are assigned to the C18—O20, C1—O25, C30—O41, C5—O6, C29—O39 and C26—O25 stretching modes. Note that the glycosidic bonds, these are the C1—O25 and C26—O25 bonds are predicted at 1025/1018 and 820/818 cm^{-1} and, hence, they were assigned at 1146 and 1017 cm^{-1}, as can be seen in Table 2. In general, the assignments of these modes presented here for both forms are in accordance with that proposed by Synytsya et al. [6] and with the predicted for three units of the galacturonic acid.

4.6.3. 1000–10 cm^{-1} region

In the previous vibrational study proposed by Synytsya et al. [6] for different pectins in this region few modes were assigned. Thus, the in-plane (805/741 cm^{-1}) and out-of-plane COO (710/575 cm^{-1}) deformation, rocking (484/396 cm^{-1}) and twisting (88–48 cm^{-1}) modes, the CH_3 (182/119 cm^{-1}) and OH twisting (554–201 cm^{-1}) modes, the corresponding deformation (1116/233 cm^{-1}) and torsion (1090/60 cm^{-1}) of both rings and, the CCO (500/101 cm^{-1}) and C—O—C (349/40 cm^{-1}) deformation modes for **Ac** and **Es** are expected in this region. Those modes related to the COO groups can be easily assigned in accordance with the calculations performed here and with related molecules [36,39], as observed in Table 2. The CH_3 twisting modes, as expected and in accordance with similar molecules [39,42] are predicted by calculations in the lower wavenumbers region, thus, these modes are associated with Raman bands observed between 144 and 119 cm^{-1}. The C—O—C deformation modes related to the glycosidic angle, in **Ac** is predicted by the SQM calculations with a PED contribution of 10% at 30 cm^{-1} while in **Es** that mode is predicted with a PED contribution of 9% at 33 cm^{-1}, for this reason, these modes could not

Table 2
Observed and calculated wavenumbers (cm^{-1}) and assignments for 6-nitro-1,3-benzothiazole-2(3*H*)-thiol and their tautomer in gas phase.

Experimental[a]		H-Pec[b]		K-Pec[b]		Assignment[b]	Ac GAS[a]		Ac PCM[a]		Es GAS[a]		Es PCM[a]		Three units[a] Gas	
IR	Ra	Ra	IR	Ra	IR		SQM[c]	Assignment	SQM[c]	Assignment	SQM[c]	Assignment	SQM[c]	Assignment	Calc[d]	Assignment
							3598	νO17—H10	3579	νO39—H40	3597	νO17—H10	3578	νO17—H10	3752	νO—H
							3590	νO16—H14	3573	νO17—H10	3588	νO16—H14	3572	νO45—H46	3743	νO—H
							3579	νO39—H40	3569	νO16—H14	3580	νO43—H44	3570	νO16—H14	3737	νO—H
							3538	νO41—H42	3558	νO41—H42	3545	νO45—H46	3568	νO15—H11	3726	νO—H
	3373s						3526	νO35—H46	3525	νO44—H45	3530	νO48—H49	3564	νO43—H44	3683	νO—H
3436vs	3301vs		3493		3425	νO—H	3498	νO44—H45	3510	νO35—H46	3486	νO15—H11	3525	νO48—H49	3676	νO—H
							3480	νO15—H11	3427	νO15—H11	3054	ν_aCH_3(C21)	3072	ν_aCH_3(C21)	3631	νO—H
	3188m						3055	ν_aCH_3	3072	ν_aCH_3	3051	ν_aCH_3(C36)	3070	ν_aCH_3(C36)	3188	ν_aCH_3
	3027w						3027	ν_aCH_3	3044	ν_aCH_3	3026	ν_aCH_3(C21)	3045	ν_aCH_3(C21)	3123	νC—H
	2984w						2983	νC26—H32	3003	νC26—H32	3023	ν_aCH_3(C36)	3041	ν_aCH_3(C36)	3109	νC—H
	2970w						2974	νC31—H43	2990	νC4—H12	3008	νC26—H32	3009	νC26—H32	3095	νC—H
	2965w						2967	νC5—H13	2989	νC31—H43	2990	νC31—H47	2988	νC31—H47	3089	νC—H
							2961	νC4—H12	2979	νC29—H38	2965	νC4—H12	2969	νC29—H42	3085	νC—H
	2957w						2958	νC1—H7	2971	νC5—H13	2960	νC5—H13	2967	νC5—H13	3084	νC—H
2950sh							2953	ν_sCH_3	2970	νC1—H7	2952	ν_sCH_3(C21)	2965	νC1—H7	3082	ν_sCH_3
	2947w	2941	2942	2945	2941	νC—H	2946	νC29—H38	2964	ν_sCH_3	2950	ν_sCH_3(C36)	2964	ν_sCH_3(C21)	3080	ν_sCH_3
2927w	2937w						2939	νC27—H33	2959	νC27—H33	2948	νC1—H7	2963	νC27—H33	3066	νC—H
2911sh	2927w						2936	νC2—H8	2957	νC2—H8	2943	νC29—H42	2962	ν_sCH_3(C36)	3061	νC—H
	2906w						2892	νC30—H37	2927	νC3—H9	2935	νC2—H8	2934	νC30—H41	3050	νC—H
2852vw	2871w						2882	νC3—H9	2921	νC30—H37	2934	νC27—H33	2933	νC4—H12	3036	νC—H
											2886	νC30—H41	2922	νC2—H8	3020	νC—H
			2653			$\nu(OH)_{COOH}$					2880	νC3—H9	2897	νC3—H9	3007	νC—H
1743s		1740	1762			$\nu(C{=}O)_{COOH}$	1769	νC34—O36	1696	νC34—O36	1764	νC18—O19	1692	νC18—O19	1845	νC=O
1640s	1697vw		1645			δH_2O	1765	νC18—O19	1689	νC18—O19	1752	νC34—O40	1685	νC34—O40	1832	νC=O
	1588vw			1607	1633	ν_{as}(COO—)									1829	νC=O
	1463vw						1461	$\delta_{as}CH_3$	1440	$\delta_{as}CH_3$	1461	$\delta_{as}CH_3$(C36)			1535	$\delta_{as}CH_3$
1458sh											1461	$\delta_{as}CH_3$(C21)			1471	ρC—H
1452sh							1447	$\delta_{as}CH_3$			1448	$\delta_{as}CH_3$(C36)	1445	ρC1—H7	1451	ρC—H
1442w	1443sh						1444	ρ′C1—H7	1437	ρC1—H7	1447	$\delta_{as}CH_3$(C21)	1439	$\delta_{as}CH_3$(C36)	1440	ρC—H
1440m							1434	δO5—H11	1434	$\delta_{as}CH_3$	1438	ρ′C1—H7	1438	ρ′C29—H42		
1440m							1433	νC30—C29	1431	ρ′C29—H38	1432	ρC30—H41	1437	$\delta_{as}CH_3$(C21)		
	1430sh						1425	ρC31—H43	1427	δ_sCH_3	1431	ρC4—H12	1435	$\delta_{as}CH_3$(C36)		
1420sh	1420sh						1425	δ_sCH_3	1422	ρC4—H12			1430	$\delta_{as}CH_3$(C21)		
											1426	δ_sCH_3(C36)	1429	δ_sCH_3(C36)	1429	ρC—H
1420sh	1420sh										1424	δ_sCH_3(C21)	1422	δ_sCH_3(C21)	1425	ρC—H
1420sh	1420sh						1417	ρ′C3—H9	1416	ρC31—H43	1418	ρ′C30—H41	1417	ρ′C3—H9	1420	ρC—H
1406sh	1408sh			1405	1419	ν_s(COO—)	1407	ρ′C30—H37	1408	ρ′C3—H9	1413	ρ′C3—H9	1408	ρC31—H47	1415	ρC—H
													1406	ρC4—H12	1404	ρC—H
		1393	1403			δCOH_{COOH}			1396	ρC29—H38	1399	ρC31—H47	1399	ρC29—H42	1401	ρC—H
													1395	ρ′C4—H12	1395	ρC—H
1383sh							1387	ρC30—H37	1384	ρ′C30—H37	1384	ρC29—H42			1387	ρC—H
	1375sh						1379	ρC2—H8	1380	ρC2—H8	1379	ρC2—H8	1380	ρ′C30—H41	1375	ρC—H
									1372	ρC26—H32			1373	ρC26—H32	1371	ρC—H
							1368	ρC1—H7	1369	ρC30—H37	1368	ρC1—H7	1369	ρC2—H8		
1366sh							1365	ρC29—H38			1365	ρC27—H33			1365	ρC—H
							1362	ρC26—H32	1362	ρC5—H13	1361	ρC26—H32	1363	ρ′C1—H7		
	1357sh						1358	ρC5—H13	1353	ρC3—H9	1356	ρC5—H13	1351	ρC30—H41	1351	ρC—H
1344sh	1344sh						1344	ρC3—H9	1346	ρ′C29—H38					1349	ρC—H
										ρC27—H33						
							1340	ρ′C29—H38	1343	ρ′C1—H7	1343	ρC3—H9	1343	ρC5—H13		
1333m	1333vs	1330	1335	1324	1334	δ(CH)					1331	ρ′C29—H42	1337	ρC27—H33		
							1322	ρC27—H33	1327	ρC27—H33			1333	ρC3—H9	1333	ρC—H
ρ	1313sh						1317	ρ′C4—H12	1320	ρ′C2—H8	1317	ρ′C4—H12	1319	ρ′C31—H47	1319	ρC—H
	1300sh						1303	ρ′C26—H32			1301	ρ′C26—H32	1307	ρ′C27—H33	1307	ρC—H
1297sh	1291sh								1299	ρ′C26—H32	1294	ρ′C27—H33	1295	ρ′C26—H32	1297	δO—H

1297sh							1287	νC26—C31	1287	ρ′C31—H43			1291	ρ′C5—H13 ρ′C26—H32	1290	δO—H
							1281	ρC4—H12	1280	δO5—H11	1280	δO5—H11				
							1273	δO44—H45	1277	ρ′C5—H13	1275	ρ′C31—H47				
1265m	1269sh						1269	ρ′C5—H13	1263	ρ′C27—H33	1270	ρ′C5—H13			1265	δO—H
	1261sh						1256	ρ′C27—H33			1257	δO48—H49	1256	δO48—H49	1261	δO—H
1253sh		1254	1253sh	1242	1236	δ(CH)			1245	δO44—H45	1239	δO45—H46	1247	ρ′C5—H13	1252	δO—H
1235m			1226			$\delta(OH)_{COOH}$	1238	δO41—H42	1232	δO41—H42	1224	νC18—O20 ρ′C5—H13	1223	δO5—H11	1229	ρCH_3
1235m							1223	νC18—O20	1220	ρ′C4—H12	1211	νC34—O35 ρ′C27—H33	1219	νC34—O35	1223	ρCH_3
1211sh							1208	δO16—H14	1209	νC18—O20	1209	νC18—O20	1200	δO17—H10 ρ′C2—H8	1210	νC—Oglyc
	1207sh						1196	δO39—H40					1198	νC29—O43	1199	νC—O
							1192	ρ′C2—H8	1192	ρCH_3	1191	ρ′C2—H8	1193	ρCH_3(C36)	1191	ρCH_3
									1186	δO17—H10	1188	ρCH_3(C36)	1191	νC18—O20	1190	ρCH_3
	1180sh						1185	ρCH_3	1185	δO39—H40	1186	δO43—H44	1187	ρCH_3 (C21)	1184	ρCH_3
	1180sh										1185	ρCH_3 (C21)	1181	δO16—H14		
	1180sh						1177	δO17—H10	1176	δO16—H14	1178	δO17—H10	1177	δO45—H46	1171	νC—Oglyc
1146s	1170sh						1174	νC1—O25	1155	νC1—O25	1161	νC1—O25	1162	δO43—H44	1155	νC—Oglyc
1146s	1152vw						1153	ρ′CH_3	1153	ρ′CH_3	1153	ρ′CH_3(C36)	1151	ρ′CH_3(C36)	1150	νC—Oglyc
1146s		1145	1156	1144	1146	ν(COC)glyc					1153	ρ′CH_3 (C21)	1150	νC1—O25	1149	νC—O
1146s	1142vw						1138	δO35—H46 νC34—O35	1143	νC29—O39	1129	νC30—O45	1148	ρ′CH_3 (C21)	1144	νC—O
1103s	1130sh						1132	νC27—O28	1116	δO35—H46 νC34—O35	1116	βR_1 (A6)	1112	νC2—O17	1125	νC—O
1103s							1121	νC30—O41							1113	νC—O
1103s		1105	1119	1106	1112	νC—C, νC—O	1109	νC4—C5	1103	νC2—O17	1110	νC5—O6 νC4—C5			1109	νC—O
1103s	1098sh						1097	νC31—O44	1094	νC5—O6	1090	νC26—C31	1091	νC26—C27 νC26—C31	1099	νC—O
1076s	1093vw						1089	νC5—O6	1088	νC30—O41	1090	νC3—O16 τR_1 (A6)	1089	νC27—O28	1097	νC—O
1076s		1079	1085	1078	1083	νC—O + δOH			1082	νC3—O16	1083	νC31—O48	1085	νC30—O45	1082	νC—O
							1075	νC26—C27	1072	νC26—C27			1080	νC5—O6	1079	νC—C
	1070vw						1068	νC4—O15			1067	νC4—O15	1064	νC4—O15	1068	νC—C
							1059	νC3—O16	1055	νC26—C31	1060	νC3—O16	1054	νC31—O48	1052	νC—C
1047s	1046vw	1050		1049		νC—C,νC—O	1052	νC29—O39	1051	νC31—O44	1049	νC29—O43	1044	νC2—C3		
	1040vw						1040	δO16—H14	1040	νC2—C3	1040	δO16—H14			1036	νC—C
									1035	νC4—O15			1035	νC3—O16	1032	νC—C
1017s	1026vw	1030	1034	1033	1036sh	νC—C,νC—O	1025	νC26—O25	1018	νC26—O25	1025	νC26—O25	1019	νC26—O25	1023	νC—O
1001sh	1003vw	990	990sh			γCOOHdim					1004	νC36—O35 νC27—C34	1002	νC1—O6	1018	νC—O
				992	992	δ(COO—)	993	νC2—C3	994	νC1—C2	1002	νC1—O6	997	νC36—O35 νC27—C34	994	νC—O
	986vw						982	νC21—O20	984	νC29—O28 νC30—C29	983	νC21—O20	976	νC21—O20	967	βR_1 (A6)
972sh	966vw						972	νC29—O28	970	νC5—C18	972	νC26—O25	967	νC5—C18	964	νC—O
953w	950vw	953	954	957	958	δ(CCH) δ(COH)	969	νC29—O28 δO28C29O39	955	νC29—O28	965	νC29—O28	956	νC29—O28	952	νC—O
938sh	937vw						942	βR_1 (A6)	940	βR_1 (A6)	942	βR_1 (A6) νC2—C3	940	βR_1 (A6)	944	νC—C
929vw	926vw						928	νC5—C18	922	νC21—O20	924	νC5—C18	919	δO6C5C18	921	δOCC
911vw	905sh		915		917		903	νC27—C34	908	νC27—C34					916	νC—O
894sh	895sh						893	νC27—O28 νC30—C29	895	νC30—C29	893	νC30—C29	899	νC30—C29	904	νC—O
889w	889sh	887	888	896	894	δ(CCH) δ(COH)	880	νC1—O6	883	νC1—O6	888	νC26—C27	886	νC36—O35 νC34—O35	889	νC—C
878sh	880sh										882	νC34—O35	881	νC1—O6	871	νC—C

(*continued on next page*)

Table 2 (*continued*)

Experimental[a]		H-Pec[b]		K-Pec[b]		Assignment[b]	Ac GAS[a]		Ac PCM[a]		Es GAS[a]		Es PCM[a]		Three units[a] Gas	
IR	Ra	Ra	IR	Ra	IR		SQM[c]	Assignment	SQM[c]	Assignment	SQM[c]	Assignment	SQM[c]	Assignment	Calc[d]	Assignment
												δO28C27C34		νC3—C4		
873sh	871sh						873	νC2—O17	865	δO25C1C2	865	νC2—O17 δO25C1C2	865	νC2—O17	865	νC—C
	849sh	853			857	(CCOCO)							858	νC4—C5		
847w	837s						848	νC3—C4	852	νC3—C4 νC4—C5	851	νC3—C4			844	βR_1 (A6)
833w	831sh	834									820	νC1—C2	820	νC1—C2	822	βR_1 (A6)
	821sh						818	νC1—C2	816	νC1—O6						
805sh	805sh						792	βR_1 (A6)	798	νC27—O28 βR_1 (A6)	802	νC27—O28	808	βR_1 (A6)	786	δCOO
782sh	784sh	795	790	814	815	γ(COH)ring	771	δCOO_{Es}	768	δCOO_{Es}	778	δCOO_{Es1}	777	δCOO_{Es1}	782	δCOO
769sh	767sh	775	760sh	774	769	Ring breezing					771	δCOO_{Es2}	771	δCOO_{Es2}		
741 w	744w	750sh	738			$\gamma(COH)_{COOH}$	716	δO17C2C1	720	νC1—O6 δO17C2C1					737	δCOO
	735w										711	δO17C2C1	708	δO17C2C1 νC36—O35	726	δOCC
704sh	707vw	710	700sh	717	710sh	γ(COH)ring	699	γCOO_{Ac}	701	νC30—C31	699	νC30—C31	699	νC30—C31	710	βR_3 (A6)
697sh	688vw	686	682	687	673	Pyranoid ring	693	νC30—C31 βR_3 (A6)	695	βR_3 (A6)					674	τOH
670w	676w										657	δO25C26C31	661	δO25C26C31	658	γCOO
635m	637vw						636	δCOO_{Ac}	638	δCOO_{Ac}					646	βR_3 (A6)
620m	620vw	621	637	636	649		634	τO35—H46	621	γCOO_{Ac}	619	γCOO_{Es2}	624	γCOO_{Es2}	633	γCOO
603w	612vw						611	γCOO_{Es}	600	γCOO_{Es}					619	τOH
	591vw						593	δO16C3C4	590	βR_2 (A6)	593	δO43C29C30	594	γCOO_{Es1} δO43C29C30	597	τOH
588w	583vw								585	δO28C29O39	591	βR_2 (A6) δO16C3C2	589	βR_2 (A6)		
588w	583vw												587	δO28C29O43	585	βR_2 (A6)
576w	575vw						579	δO28C29O39			579	γCOO_{Es1} δO28C29O43				
554sh	556vw						549	τO15—H11	543	τO15—H11 τO35—H46	543	τO15—H11			542	βR_2 (A6)
536w	545vw	537	534	538	544		545	τO15—H11 τO35—H46	540	τO35—H46					539	τOH
526w	524vw						525	τO15—H11	517	τO15—H11	525	βR_3 (A6) δO25C1O6	528	νC3—C4	526	βR_2 (A6)
508w	507vw						514	δO25C1O6	512	δO25C1O6	517	δO17C2C3	517	δO25C1O6	524	βR_3 (A6)
490w	491vw										494	δO45C30C31			492	τOH
484w	485vw	486		483			484	ρCOO_{Ac}	484	δC30C31O44			484	βR_3 (A6)	467	τOH
474m	475vw										471	τO48—H49				
466m	465vw						467	τO44—H45 τO41—H42								
455m	453vw								451	τR_1 (A6)	451	ρCOO_{Es1}	450	δC30C31O48	447	τOH
444sh	444vw	441		444		τC—O—C	444	βR_3 (A6)					441	βR_2 (A6)	440	τOH
440m	435sh						437	βR_2 (A6)	439	δO16C3C2	437	βR_2 (A6)				
429m	430vw						432	δO16C3C2 δO17C2C3	431	ρCOO_{Ac}	432	δO16C3C2	434	δO16C3C2	431	δOCC
416w	412w						415	βR_2 (A6)	410	ρCOO_{Es}	413	δC30C31O48	414	ρCOO_{Es2} δO16C3C4	415	τOH
405w	396vw						395	τO39—H40	398	δO17C2C3 δC26C31O44	394	ρCOO_{Es2}	396	δO17C2C3	404	ρCOO
	390sh								389	τO39—H40					392	δOCC
	383sh						380	τO41—H42	382	τO44—H45	378	τO45—H46	380	δO25C26C27	383	δOCC
	378w	372		378			377	τO44—H45	373	δO25C26C27	373	τO43—H44	370	βR_2 (A6)	378	τOH
	368w						362	τO44—H45			363	βR_2 (A6)	358	τO43—H44 δO6C5C18	363	δOCC
	357w								353	δO6C5C18	350	δO6C5C18	353	τO43—H44	353	δOCC

349sh				349	δO6C5C18	342	βR_2 (A6)	349	τO43—H44 δC34O35C36	347	τO48—H49	350	δOCC
339w	340	344	τC—O—C	330	δC30C31O44	334	δO15C4C5	329	δO15C4C3 δO15C4C5	327	δO15C4C3	322	τOH
328w				325	δO15C4C5	321	δO41C30C31	317	τO16—H14	319	δO15C4C5	319	τOH
315w				305	δO25C26C31	312	τO41—H42			310	δC34O35C36	304	δOCC
297sh				295	δC18O20C21 τR_1 (A6)	305	τO16—H14	305	δC34O35C36	298	δC18O20C21	299	δCOC
293w				290	τO16—H14	298	τO17—H10	295	τO16—H14			296	τO—H
						292	δC18O20C21	291	δC18O20C21	289	τO45—H46	283	τO—H
284w				284	δO41C30C31 δC26C31O44					280	δC26C31O48 δO45C30C31	281	δOCC
273sh				273	δO28C27C34	271	δO28C27C34	270	δC26C31O48	269	τO16—H14	268	τO—H
261w						268	δO39C29C30 βR_3 (A6)			267	δO45C30C29	258	τO—H
255sh				258	δO41C30C29 δO39C29C30			258	δO16C3C4	255	τO17—H10 τO16—H14	240	τO—H
247w				250	δO15C4C3	242	δO15C4C3 δO16C3C4	247	δO45C30C29				
233sh				226	τR_2 (A6)	233	δO41C30C29	234	βR_3 (A6)	239	δO28C27C34 ρCOO_{Es1}	238	δOCC
224w				221	τO17—H10			224	τO15—H11 τO17—H10	225	τO17—H10	230	τR_1 (A6)
218w						213	δO17C2C1	209	τO17—H10	211	δO17C2C1	213	τR_1 (A6)
201w				195	τO17—H10	200	δC18C5C4	192	τO17—H10	195	τR_2 (A6)	205	τR_1 (A6)
182w				174	δO25C1C2 ρCOO_{Es}	175	τwCH_3	173	τR_1 (A6)	179	τR_1 (A6)	181	τR_2 (A6)
173w				163	τR_1 (A6)	168	δC26C27C34	161	τR_1 (A6)	161	δO25C1C2	164	τR_2 (A6)
150w				151	τO20—C21	155	τR_1 (A6)	152	τO20—C21	152	τO20—C21 τR_1 (A6)	151	τwCH_3
144w				144	τR_2 (A6)	146	τR_1 (A6)			147	τwCH_3(C36)	147	τR_2 (A6)
						138	τR_2 (A6)	139	τwCH_3(C36)	139	τO15—H11	140	τwCH_3
136vw				126	τwCH_3			137	τR_2 (A6)	133	τO15—H11	133	τR_3 (A6)
126sh								125	τO35—C36	129	τwCH_3(C21)	121	τR_3 (A6)
119w				121	δC26C27C34	117	τR_2 (A6)	121	τwCH_3(C21)	125	τO35—C36		
113sh				109	δC18C5C4	110	τO20—C21	108	δC18C5C4	105	δC26C27C34	114	τR_3 (A6)
101w				103	δO25C26C27			102	δC26C27C34	104	δC18C5C4	113	δCCC
97sh				90	τR_3 (A6)	97	τR_3 (A6) δO25C26C31					95	δCCC
88w						83	τR_3 (A6)	86	τR_2 (A6)	84	τR_2 (A6)	85	τwCOO
75sh				72	τR_3 (A6)			81	τR_3 (A6)	79	τR_3 (A6)	73	τwCOO
69sh						67	τR_3 (A6) τR_2 (A6)	60	τR_3 (A6)	62	$\tau wCOO_{Es1}$	64	τwCOO
55sh				53	$\tau wCOO_{Ac}$	56	$\tau wCOO_{Ac}$	53	$\tau wCOO_{Es1}$	60	τR_3 (A6)	55	δCOC
				48	$\tau wCOO_{Es}$	48	$\tau wCOO_{Es}$	49	$\tau wCOO_{Es2}$	46	$\tau wCOO_{Es2}$	44	δCOC
				41	τw(A6)	35	τw(A6) δC1O25C26			37	δC1O25C26	37	δCOC
				30	δC1O25C26	32	τw(A6)	33	δC1O25C26			30	τw(A6)
								24	τw(A6)	26	τw(A6)	15	τw(A6)
				12	τw(A6)	15	τw(A6)	10	τw(A6) δO25C26C27	22	τw(A6)	11	τw(A6)

ν, stretching; δ, scissoring; γ, wagging or out-of-plane deformation; ρ, rocking; τ, torsion; τw, twisting; a, antisymmetric; s, symmetric; ip, in-phase; op, out-of-phase; R, ring; benzene ring, (A6); thiazole ring, (A5); Sym, symmetry.

[a] This work.

[b] From Ref [6].

[c] From scaled quantum mechanics force field B3LYP/6-31G*.

[d] From B3LYP/6-31G* level.

Table 3
Scaled force constants for both structures proposed of pectin in gas and aqueous solution by using B3LYP/6-31G* method.

B3LYP/6-31G*							
Force constant	Gas[a]	PCM[a]	Gas[a]	PCM[a]	Gas[b]	PCM[b]	Gas[c]
$f(\nu O{-}H)$	7.03	6.99	7.07	7.10	7.186	7.062	6.10
$f(\nu CH_3)/f(\nu CH_2)$	5.00	5.05	5.00	5.04	4.767	4.812	5.34
$f(\nu C{-}H)$	4.77	4.84	4.78	4.81	4.723	4.728	5.69
$f(\nu C{=}O)$	12.49	11.56	12.42	11.52			13.65
$f(\nu C{-}O)_C$	4.64	4.51	4.63	4.53	4.460	4.266	
$f(\nu C{-}O)_H$	5.13	5.13	5.07	5.08	4.976	4.895	6.36
$f(\nu C{-}C)_{R6/R5}$	3.77	3.85	3.78	3.90	3.868	3.855	
$f(\nu C{-}C)_{R6}$	3.93	3.93	3.93	3.93	3.965	3.965	6.65
$f(\delta C{-}O{-}C)$	1.32	1.20	1.13	1.31	1.728	1.299	
$f(\delta\ C{-}O{-}H)$	0.77	0.75	0.77	0.74	0.733	0.741	1.06
$f(\delta CH_3)/f(\delta CH_2)$	0.57	0.56	0.57	0.56	0.803	0.796	0.91

Units are mdyn $Å^{-1}$ for stretching and stretching/stretching interaction and mdyn $Å\ rad^{-2}$ for angle deformations, R6, glucopyran rings according to Fig. S2.
[a] This work.
[b] For sucrose, from Ref. [7].
[c] For 5,7-Dichloro-quinolin-8-yloxy) acetic acid, from Ref. [9].

be assigned. In sucrose, the deformation mode related to the glycosidic angle was associated with a very weak Raman band at 178 cm^{-1} [9]. The other modes were assigned according to the SQM calculations, as indicate in Table 2. Clearly, the assignments proposed in this region for three units of the galacturonic acid are in accordance with those descript for two subunits, as shown Table 2.

5. Force constants

For **Ac** and **Es** in the two studied media were calculated the force constants expressed in internal coordinates by using the B3LYP/6-31G* method and the Molvib program [27]. The results are observed in Table 3 compared with those reported for sucrose [9] and a conformer of the 5,7-Dichloro-quinolin-8-yloxy) acetic acid [37]. The differences observed among the $f(\nu O{-}H)$, $f(\nu C{=}O)$ and $f(\nu C{-}O)_C$ force constant values for **Ac** and **Es** in gas phase with those in solution are obviously attributed to the hydration due to the H bonds formation. Note that only slightly modifications between the $f(\nu C{-}O)_H$ and $f(\delta C{-}O{-}C)$ force constants of **Ac** and **Es** are observed. Obviously, the $f(\nu C{-}O)_H$ value is higher in Ac because a C—O bond is linked to a H atom while in Es that bond is linked to a CH_3 group. On the other hand, the differences observed in $f(\delta C{-}O{-}C)$ are related to the geometrical parameters because they have different values, as observed in Table 1. Comparing the $f(\delta C{-}O{-}C)$ force constants, we observed that the higher values for sucrose in both media is probably related to the calculations because the deformation mode is assigned at 178 cm^{-1} while in this work the modes related to those constants for **Ac** and **Es** are predicted a low frequencies (30 and 33 cm^{-1}). The differences between the values for **Ac** and **Es** with those corresponding to 5,7-Dichloro-quinolin-8-yloxy) acetic acid [37] show clearly the differences between the force constants of a acid and a ester compound. In general, the force constants values calculated for both forms proposed are in agreement with those reported in the literature for molecules containing similar groups [9,36–39].

6. Conclusions

In this work, a pectin isolated from citrus peel with a degree of esterification of 76% was characterized by FTIR and FT-Raman spectroscopies. The polygalacturonic acid chain was studied taking into account their partial esterification's degree by simulation of two different subunits, one with both COOH and COO—CH_3 groups (**Ac**) and, the other one as constituted by two subunits with two COO—CH_3 groups (**Es**). The molecular structures of both forms were determinate in gas phase and in aqueous solution by using the hybrid B3LYP/6-31G* method. The solvent effects and the solvation energies were considered by employing the PCM/SM model. Also, three subunits formed by two COO—CH_3 and one COO groups were theoretically simulated by using the same level of theory. The observed separation of 103 cm^{-1} between the more intense IR bands suggest the presence of two C=O groups with different moieties linked to these which are —OH and —O—CH_3 while the theoretical calculations support the presence of the three structures proposed for a pectin esterified a 76%. Here, the IR bands at 3436 (OH), 1743 (C=O), 1640 (C=O), 1146 (C—O glycosidic), 1103 (C—O) and 1017 (C—O glycosidic) cm^{-1} characterizing clearly a pectin. The infrared and Raman spectra for these three structures proposed show a reasonable concordance with the experimental ones. The two structures proposed show clear differences in the dipole moments and solvation energy values in solution. The molecular electrostatic potential reveals the different sites of H bonds formation while the MK charges on the COO groups show clear differences between the two structures in solution. The NBO study suggest that **Ac** is most stable than **Es** while the AIM analyses show four different interactions for **Ac** in gas phase and five interactions in the same phase, some of which disappear in solution as a consequence of the hydration. This study provides a new insight to study the interactions that exist between subunits of a large pectin chain and, besides, it work will allow the quick identification of pectin by using the vibrational spectroscopy.

Acknowledgements

This work was supported with grants from CIUNT (Consejo de Investigaciones, Universidad Nacional de Tucumán). Dr. Gervasi is a Researcher at CICPBA and INQUINOA. The authors would like to thank Prof. Tom Sundius for his permission to use MOLVIB and to INQUINOA (CONICET) for the spectra.

Appendix A. Supplementary material

Supplementary data associated with this article can be found, in the online version, at http://dx.doi.org/10.1016/j.infrared.2016.03.009.

References

[1] P. Sriamornsak, Chemistry of pectin and its pharmaceutical uses: a review, silpakorn university, J. Soc. Sci. Human. Arts 3 (1–2) (2003) 206–228.
[2] Colin D. May, Industrial pectins: sources, production and applications, Carbohyd. Polym. 12 (1) (1990) 79–99.
[3] William G.T. Willats, J. Paul Knox, Jørn Dalgaard Mikkelsen, Trends Food Sci. Technol. 17 (3) (2006) 97–104.
[4] T.P. Kravtchenko, A.G.J. Voragen, W. Pilnik, Analytical comparison of three industrial pectin preparations, Carbohyd. Polym. 18 (1) (1992) 17–25.
[5] Hai-ming Chen, Xiong Fu, Zhi-gang Luo, Properties and extraction of pectin-enriched materials from sugar beet pulp by ultrasonic-assisted treatment combined with subcritical water, Food Chem. 168 (2015) 302–310.
[6] A. Synytsya, J. Čopıková, P. Matějka, V. Machovič, Fourier transform Raman and infrared spectroscopy of pectins, Carbohyd. Polym. 54 (2003) 97–106.
[7] A.B. Brizuela, A.B. Raschi, M.V. Castillo, P. Leyton, E. Romano, S.A. Brandán, Comparison between the structural and vibrational properties of the artificial sweetener sucralose with those obtained for sucrose, Comput. Theor. Chem. 1008 (2013) 52–60.
[8] A.B. Brizuela, L.C. Bichara, E. Romano, A. Yurquina, S. Locatelli, S.A. Brandán, A complete characterization of the vibrational spectra of sucrose, Carbohyd. Res. 361 (2012) 212–218.
[9] A.B. Brizuela, M.V. Castillo, A.B. Raschi, L. Davies, E. Romano, S.A. Brandán, A complete assignment of the vibrational spectra of sucrose in aqueous medium based on the SQM methodology and SCRF calculations, Carbohyd. Res. 388 (2014) 112–124.
[10] M.V. Fiori-Bimbi, P.E. Alvarez, H. Vaca, C.A. Gervasi, Corrosion inhibition of mild steel in HCL solution by pectin, Corros. Sci. (2015), http://dx.doi.org/10.1016/j.corsci.2014.12.002.

[11] A.D. Becke, Density functional thermochemistry. III. The role of exact exchange, J. Chem. Phys. 98 (1993) 5648–5652.
[12] C. Lee, W. Yang, R.G. Parr, Development of the Colle–Salvetti correlation-energy formula into a functional of the electron density, Phys. Rev. B 37 (1988) 785–789.
[13] J. Tomasi, J. Persico, Molecular interactions in solution: an overview of methods based on continuous distributions of the solvent, Chem. Rev. 94 (1994) 2027–2094.
[14] S. Miertus, E. Scrocco, J. Tomasi, Electrostatic interaction of a solute with a continuum. A direct utilization of ab initio molecular potentials for the prevision of solvent effects, Chem. Phys. 55 (1981) 117–129.
[15] (a) G. Rauhut, P. Pulay, Transferable scaling factors for density functional derived vibrational force fields, J. Phys. Chem. 99 (1995) 3093–3100;
(b) G. Rauhut, P. Pulay, J. Phys. Chem. 99 (1995) 14572.
[16] A.B. Nielsen, A.J. Holder, Gauss View 5.0, User's Reference, GAUSSIAN Inc., Pittsburgh, PA, 2000–2008.
[17] A.V. Marenich, C.J. Cramer, D.G. Truhlar, Universal solvation model based on solute electron density and a continuum model of the solvent defined by the bulk dielectric constant and atomic surface tensions, J. Phys. Chem. B 113 (2009) 6378–6396.
[18] L.C. Bichara, S.A. Brandán, Hydration of species derived from ascorbic acid in aqueous solution. An experimental and theoretical study by using DFT calculation, J. Mol. Liq. 181 (2013) 34–43.
[19] A.B. Brizuela, A.B. Raschi, M.V. Castillo, L. Davies, E. Romano, S.A. Brandán, Vibrational investigation on species derived from cyclamic acid in aqueous solution by using HATR and Raman spectroscopies and SCRF calculations, J. Mol. Struct. 1074 (2014) 144–156.
[20] M.J. Frisch, G.W. Trucks, H.B. Schlegel, G.E. Scuseria, M.A. Robb, J.R. Cheeseman, G. Scalmani, V. Barone, B. Mennucci, G.A. Petersson, H. Nakatsuji, M. Caricato, X. Li, H.P. Hratchian, A.F. Izmaylov, J. Bloino, G. Zheng, J.L. Sonnenberg, M. Hada, M. Ehara, K. Toyota, R. Fukuda, J. Hasegawa, M. Ishida, T. Nakajima, Y. Honda, O. Kitao, H. Nakai, T. Vreven, J.A. Montgomery, Jr., J.E. Peralta, F. Ogliaro, M. Bearpark, J.J. Heyd, E. Brothers, K.N. Kudin, V.N. Staroverov, R. Kobayashi, J. Normand, K. Raghavachari, A. Rendell, J.C. Burant, S.S. Iyengar, J. Tomasi, M. Cossi, N. Rega, J.M. Millam, M. Klene, J.E. Knox, J.B. Cross, V. Bakken, C. Adamo, J. Jaramillo, R. Gomperts, R.E. Stratmann, O. Yazyev, A.J. Austin, R. Cammi, C. Pomelli, J.W. Ochterski, R.L. Martin, K. Morokuma, V.G. Zakrzewski, G.A. Voth, P. Salvador, J.J. Dannenberg, S. Dapprich, A.D. Daniels, O. Farkas, J.B. Foresman, J.V. Ortiz, J. Cioslowski, and D.J. Fox, Gaussian Inc, Wallingford CT, 2009.
[21] A.E. Reed, L.A. Curtis, F. Weinhold, Intermolecular interactions from a natural bond orbital, donor-acceptor viewpoint, Chem. Rev. 88 (6) (1988) 899–926.
[22] E.D. Glendening, J.K. Badenhoop, A.D. Reed, J.E. Carpenter, F. Weinhold, NBO 3.1; Theoretical Chemistry Institute, University of Wisconsin, Madison, WI, 1996.
[23] R.F.W. Bader, Atoms in Molecules. A Quantum Theory, Oxford University Press, Oxford, 1990. ISBN: 0198558651.
[24] F. Biegler-Köning, J. Schönbohm, D.J. Bayles, AIM2000; a program to analyze and visualize atoms in molecules, Comput. Chem. 22 (2001) 545–549.
[25] R.G. Parr, R.G. Pearson, Absolute hardness: companion parameter to absolute electronegativity, J. Am. Chem. Soc. 105 (1983) 7512–7516.
[26] B.H. Besler, K.M. Merz Jr., P.A. Kollman, Atomic charges derived from semiempirical methods, J. Comput. Chem. 11 (1990) 431–439.
[27] T. Sundius, Molvib. A flexible program for force field calculations, J. Mol. Struct. 218 (1990) 321–326.
[28] P. Ugliengo, MOLDRAW Program, University of Torino, Dipartimento Chimica IFM, Torino, Italy, 1998.
[29] D. Lamba, G. Fabrizi, B. Matsuhiro, Methyl-α-D-galacturonic acid methyl ester, Acta Cryst. C50 (1994) 1494–1497.
[30] I.S. Bushmarinov, K.A. Lyssenko, M. Yu Antipin, Atomic energy in the 'Atoms in Molecules' theory and its use for solving chemical problems, Russ. Chem. Rev. 78 (4) (2009) 283–302.
[31] S.A. Brandán, A. Ben Altabef, E.L. Varetti, Spectroscopic and thermal properties of chromyl acetato and trifluoroacetate, Anal. Asoc. Qca. Arg. 87 (1,2) (1999) 89–96.
[32] S.A. Brandán, Volume 2: A Structural and Vibrational Investigation into Chromylazide, Acetate, Perchlorate, and Thiocyanate Compounds, Editado by Ken Derham, Springer Science, Business Media B.V., Van Godewijckstraat 30, 3311 GZ Dordrecht, Netherlands, September 2012, 84 pág (ISBN: 978-94-007-5753-0).
[33] C.D. Contreras, A.E. Ledesma, H.E. Lanús, J. Zinczuck, S.A. Brandán, Hydration of L-tyrosine in aqueous medium. An experimental and theoretical study by mixed quantum mechanical/molecular mechanics methods, Vibrat. Spectr. 57 (2011) 108–115.
[34] P. Leyton, J. Brunet, V. Silva, C. Paipa, M.V. Castillo, S.A. Brandán, An experimental and theoretical study of L-tryptophan in aqueous solution combining two-layered ONIOM and SCRF calculations, Spectrochim. Acta, Part A 88 (2012) 162–170.
[35] Karina Guzzetti, Alicia B. Brizuela, Elida Romano, Silvia A. Brandán, Structural and vibrational study on zwitterions of L-threonine in aqueous phase using the FT-Raman and SCRF calculations, J. Mol. Struct. 1045 (2013) 171–179.
[36] Gerardo R. Argañaraz, Elida Romano, Juan Zinczuk, Silvia A. Brandán, Structural and vibrational study of 2-(8-quinolinyloxy)-acetic acid based on FTIR-Raman spectroscopy and DFT calculations, J. Chem. Chem. Eng. 5 (8) (2011) 747–758.
[37] E. Romano, M.V. Castillo, J.L. Pergomet, J. Zinczuk, S.A. Brandán, Synthesis, structural and vibrational analysis of (5,7-dichloro-quinolin-8-yloxy) acetic acid, J. Mol. Struct. 1018 (2012) 149–155.
[38] E. Romano, M.V. Castillo, J.L. Pergomet, J. Zinczuk, S.A. Brandán, Synthesis, structural study and vibrational spectra of (5-chloro-quinolin-8-yloxy) acetic acid, Open J. Synth. Theory Appl. 2 (2013) 8–22.
[39] E. Romano, J.L. Pergomet, J. Zinczuk, S.A. Brandán, Structural and vibrational properties of some quinoline acetic acid derivatives with potentials biological activities, in: Angelo Basile Edit. "Acetic Acids: Chemical Properties, Production and Applications", Edited Collection, Nova Science Publishers, 2013, pp.75–98.
[40] E. Lizarraga, E. Romano, A.B. Raschi, P. Leyton, C. Paipa, Atilio.C.N. Catalán, S.A. Brandán, A structural and vibrational study of 9,10-dihydrofukinone combining FTIR, FTRaman and NMR spectroscopies with DFT calculations, J. Mol. Struct. 1048 (2013) 331–338.
[41] Fernando Chain, Elida Romano, Patricio Leyton, Carolina Paipa, César A.N. Catalán, Mario A. Fortuna, Silvia A. Brandán, An experimental study of the structural and vibrational properties of sesquiterpene lactone cnicin using FT-IR, FT-Raman, UV–Visible and NMR spectroscopies, J. Mol. Struct. 1065–1066 (2014) 160–169.
[42] F. Chain, P. Leyton, C. Paipa, M. Fortuna, S.A. Brandán, FT-IR, FT-Raman, UV–Visible, and NMR spectroscopy and vibrational properties of the labdane-type diterpene 13-*epi*-sclareol, Spectrochim. Acta 138 (2015) 303–313.